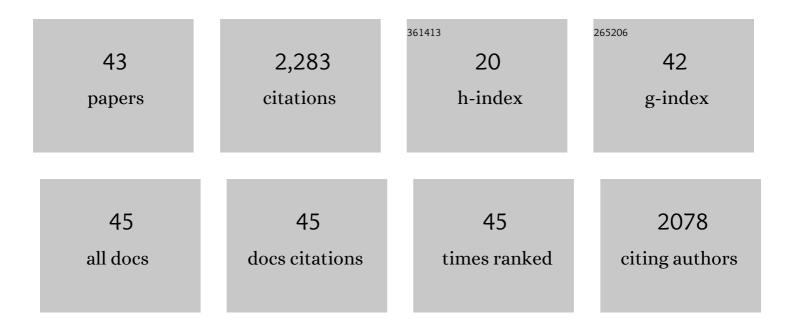
## Astrid Holzheid

List of Publications by Year in descending order

Source: https://exaly.com/author-pdf/74191/publications.pdf Version: 2024-02-01



ASTRID HOLZHEID

#	Article	IF	CITATIONS
1	Heterogeneous accretion, composition and core–mantle differentiation of the Earth. Earth and Planetary Science Letters, 2011, 301, 31-42.	4.4	352
2	Fractionation of the Platinum-Group Elements During Mantle Melting. Science, 2004, 305, 1951-1953.	12.6	266
3	Geochemical evidence for magmatic water within Mars from pyroxenes in the Shergotty meteorite. Nature, 2001, 409, 487-490.	27.8	176
4	Sulfur saturation limits in silicate melts and their implications for core formation scenarios for terrestrial planets. American Mineralogist, 2002, 87, 227-237.	1.9	164
5	Stabilities of laurite RuS2 and monosulfide liquid solution at magmatic temperature. Chemical Geology, 2004, 208, 265-271.	3.3	145
6	Evidence for a late chondritic veneer in the Earth's mantle from high-pressure partitioning of palladium and platinum. Nature, 2000, 406, 396-399.	27.8	141
7	The activities of NiO, CoO and FeO in silicate melts. Chemical Geology, 1997, 139, 21-38.	3.3	138
8	The effect of oxygen fugacity and temperature on solubilities of nickel, cobalt, and molybdenum in silicate melts. Geochimica Et Cosmochimica Acta, 1994, 58, 1975-1981.	3.9	122
9	Phase equilibria of the Shergotty meteorite: Constraints on preâ€eruptive water contents of martian magmas and fractional crystallization under hydrous conditions. Meteoritics and Planetary Science, 2001, 36, 793-806.	1.6	83
10	New Ni and Co metal-silicate partitioning data and their relevance for an early terrestrial magma ocean. Earth and Planetary Science Letters, 2008, 268, 28-40.	4.4	78
11	Solubility of copper in silicate melts as function of oxygen and sulfur fugacities, temperature, and silicate composition. Geochimica Et Cosmochimica Acta, 2001, 65, 1933-1951.	3.9	77
12	Transparent nanocrystalline bulk alumina obtained at 7.7GPa and 800°C. Scripta Materialia, 2013, 69, 362-365.	5.2	59
13	The influence of FeO on the solubilities of cobalt and nickel in silicate melts. Geochimica Et Cosmochimica Acta, 1996, 60, 1181-1193.	3.9	57
14	Textural equilibria of iron sulfide liquids in partly molten silicate aggregates and their relevance to core formation scenarios. Journal of Geophysical Research, 2000, 105, 13555-13567.	3.3	51
15	Modeling, parameterization and evaluation of monitoring methods for CO2 storage in deep saline formations: the CO2-MoPa project. Environmental Earth Sciences, 2012, 67, 351-367.	2.7	43
16	Separation of sulfide melt droplets in sulfur saturated silicate liquids. Chemical Geology, 2010, 274, 127-135.	3.3	36
17	The Crî—,Cr2O3 oxygen buffer and the free energy of formation of Cr2O3 from high-temperature electrochemical measurements. Geochimica Et Cosmochimica Acta, 1995, 59, 475-479.	3.9	32
18	High Structural Complexity of Potassium Uranyl Borates Derived from High-Temperature/High-Pressure Reactions. Inorganic Chemistry, 2013, 52, 5110-5118.	4.0	32

ASTRID HOLZHEID

#	Article	IF	CITATIONS
19	On the lower limit of chondrule cooling rates: The significance of iron loss in dynamic crystallization experiments. Meteoritics and Planetary Science, 1998, 33, 65-74.	1.6	27
20	The formation of eucrites: Constraints from metalâ€silicate partition coefficients. Meteoritics and Planetary Science, 2007, 42, 1817-1829.	1.6	24
21	Determination of the formal Ge-oxide species in silicate melts at oxygen fugacities applicable to terrestrial core formation scenarios. European Journal of Mineralogy, 2011, 23, 369-378.	1.3	17
22	Magmatic evolution of the Jbel Boho alkaline complex in the Bou Azzer inlier (Anti-Atlas/Morocco) and its relation to REE mineralization. Journal of African Earth Sciences, 2017, 129, 202-223.	2.0	16
23	Synthesis of Al <sub>2</sub> O <sub>3</sub> /SiO <sub>2</sub> nanoâ€nano composite ceramics under high pressure and its inverse Hall–Petch behavior. Journal of the American Ceramic Society, 2017, 100, 323-332.	3.8	16
24	Partial molar volumes of NiO and CoO liquids: implications for the pressure dependence of metal-silicate partitioning. Earth and Planetary Science Letters, 1999, 171, 171-183.	4.4	15
25	Synthesis of Uranium Materials under Extreme Conditions: UO <sub>2</sub> [B <sub>3</sub> Al <sub>4</sub> O <sub>11</sub> (OH)], a Complex 3D Aluminoborate. Chemistry - A European Journal, 2012, 18, 4166-4169.	3.3	15
26	Microfabric and anisotropy of elastic waves in sandstone – An observation using high-resolution X-ray microtomography. Journal of Structural Geology, 2013, 49, 35-49.	2.3	13
27	Sulphide melt distribution in partially molten silicate aggregates: implications to core formation scenarios in terrestrial planets. European Journal of Mineralogy, 2013, 25, 267-277.	1.3	11
28	The effect of metal composition on Fe–Ni partition behavior between olivine and FeNi-metal, FeNi-carbide, FeNi-sulfide at elevated pressure. Chemical Geology, 2005, 221, 207-224.	3.3	10
29	Comment on "Prediction of metal–silicate partition coefficients for siderophile elements: An update and assessment of PT conditions for metal–silicate equilibrium during accretion of the Earth―by K. Righter, EPSL 304 (2011) 158–167, 2011. Earth and Planetary Science Letters, 2011, 312, 516-518.	4.4	9
30	Dissolution kinetics of selected natural minerals relevant to potential CO2-injection sites â^' Part 1: A review. Chemie Der Erde, 2016, 76, 621-641.	2.0	8
31	Time-resolved interaction of seawater with gabbro: An experimental study of rare-earth element behavior up to 475 °C, 100 MPa. Geochimica Et Cosmochimica Acta, 2017, 197, 167-192.	3.9	8
32	Dissolution kinetics of selected natural minerals relevant to potential CO2-injection sites – Part 2: Dissolution and alteration of carbonates and feldspars in CO2-bearing brines. Chemie Der Erde, 2016, 76, 643-657.	2.0	7
33	Thermal behavior of ferric selenite hydrates (Fe2(SeO3)3·3H2O, Fe2(SeO3)3·5H2O) and the water content in the natural ferric selenite mandarinoite. Chemie Der Erde, 2018, 78, 228-240.	2.0	7
34	Transparent polycrystalline nanoceramics consisting of triclinic Al <sub>2</sub> SiO <sub>5</sub> kyanite and Al <sub>2</sub> O <sub>3</sub> corundum. Journal of the American Ceramic Society, 2018, 101, 998-1003.	3.8	6
35	Rich Coordination of Nd <sup>3+</sup> in Mg <sub>2</sub> Nd <sub>13</sub> (BO <sub>3</sub> ) <sub>8</sub> (SiO <sub>4</sub> ) <sub>4</sub> (OH) <s Derived from High-Pressure/High-Temperature Conditions. Inorganic Chemistry, 2012, 51, 3941-3943.</s 	ubx43@/sub	)>,4
36	Element signatures of subduction-zone fluids. An experimental study of the element partitioning (Dfluid/rock) of natural partly altered igneous rocks from the ODP drilling site 1,256. International Journal of Earth Sciences, 2014, 103, 1917-1927.	1.8	4

ASTRID HOLZHEID

#	Article	IF	CITATIONS
37	Multi-Scale Measurements of Neolithic Ceramics—A Methodological Comparison of Portable Energy-Dispersive XRF, Wavelength-Dispersive XRF, and Microcomputer Tomography. Minerals (Basel,) Tj ETQq1 1	<b>0.</b> 084314	14gBT ∕Over
38	Formation of solid bituminous matter in pegmatites: Constraints from experimentally formed organic matter on microporous silicate minerals. Chemie Der Erde, 2014, 74, 343-351.	2.0	3
39	A Calorimetric and Thermodynamic Investigation of the Synthetic Analogue of Mandarinoite, Fe2(SeO3)3â^™5H2O. Geosciences (Switzerland), 2018, 8, 391.	2.2	3
40	Core geophysics. Proceedings of the National Academy of Sciences of the United States of America, 1997, 94, 12742-12743.	7.1	2
41	Iron sulfide stoichiometry as a monitor of sulfur fugacity in gas-mixing experiments. American Mineralogist, 2013, 98, 1487-1496.	1.9	1
42	Expanding Family of Litharge-Derived Sulfate Minerals and Synthetic Compounds: Preparation and Crystal Structures of [Bi2CuO3]SO4 and [Ln2O2]SO4 (Ln = Dy and Ho). Minerals (Basel, Switzerland), 2020, 10, 887.	2.0	1
43	Preface: EMPG XIV. European Journal of Mineralogy, 2013, 25, 253-253.	1.3	0